FIGURE 2.1

Semilog plot of DRAM bits and minimum feature size as a function of time. (Courtesy of Dr. Rashid Bashir, Purdue University.) See also Volume I, Chapter 4.

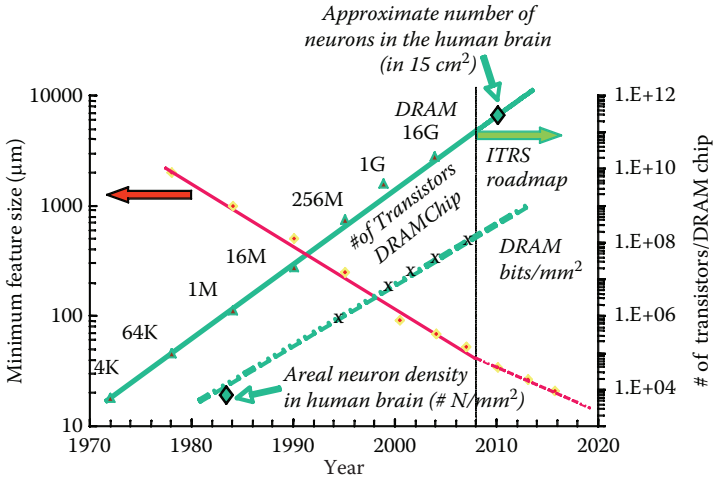

FIGURE 2.2

Ray Kurzweil is on the left, but does Bill believe him?

FIGURE 2.3

What $1000 of computing buys. The number of million instructions per second (MIPS) is a general measure of computing performance. (Based on Ray Kurzweil.)

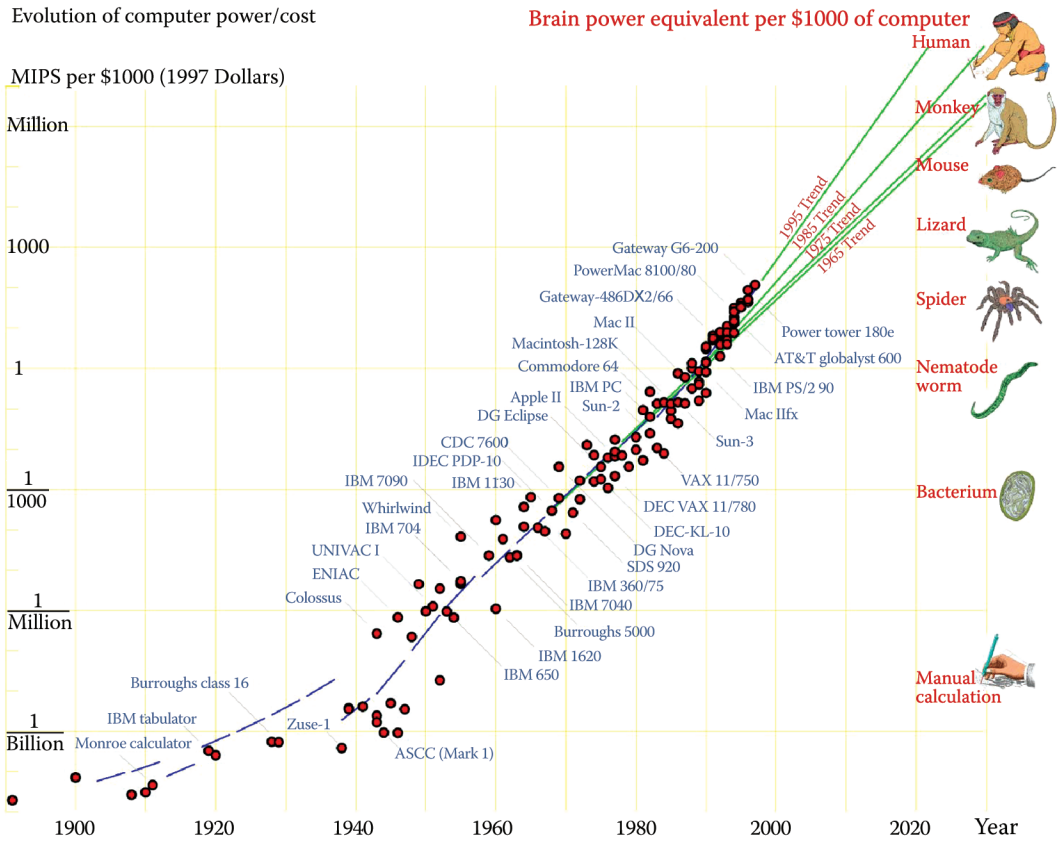

FIGURE 2.4

(a) Thin film read/write head. (b) STM-based read/write head (IBM's millipede).

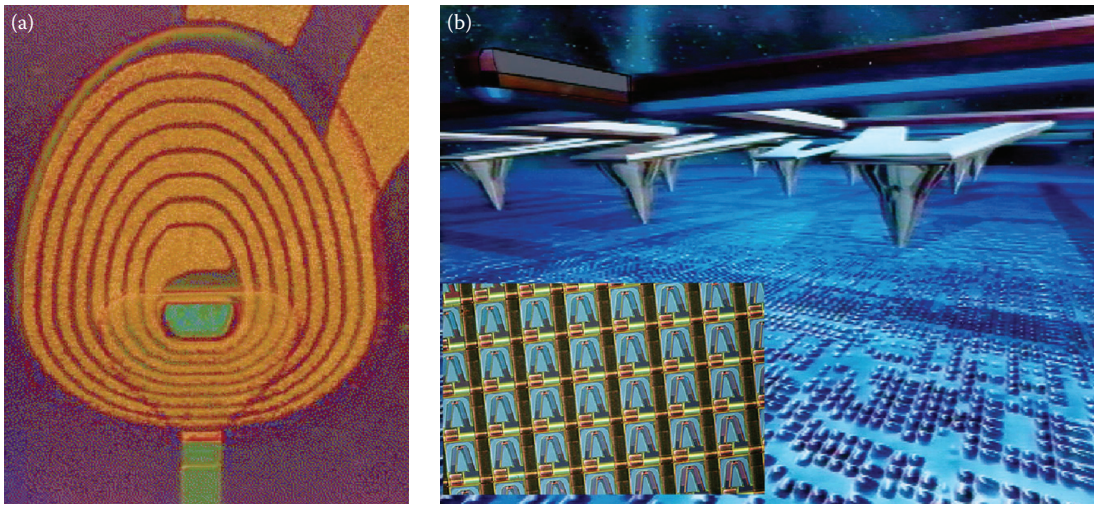

FIGURE 2.5

Schematic of an EUVL lithography setup. (From SEMATECH's Next Generation Lithography Workshop brochure.)

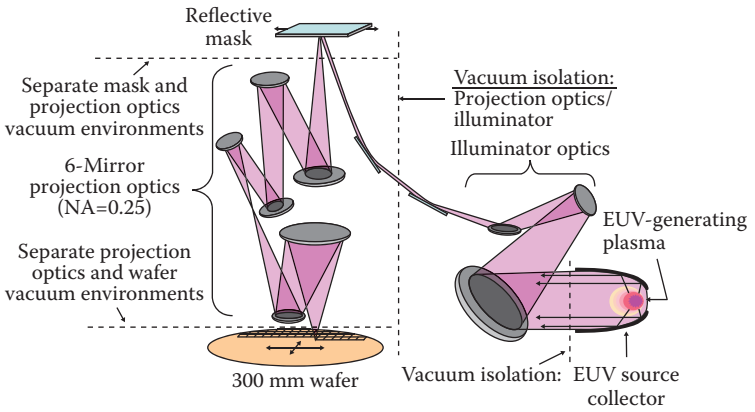

FIGURE 2.6

Two schematic representations of EUVL reflective masks. In EUVL, only reflective optics will work (see text).

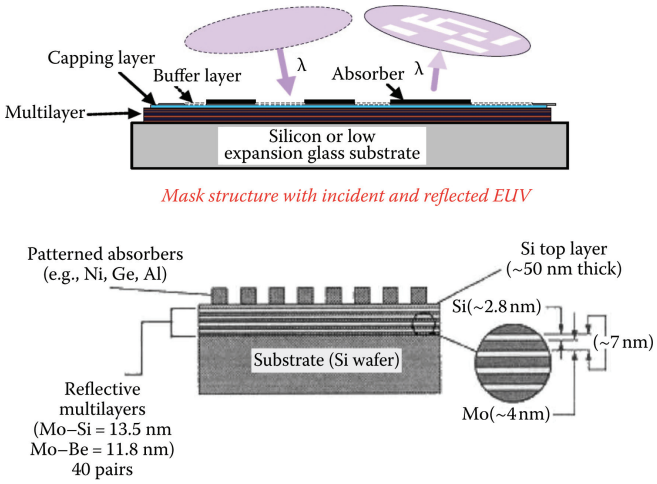

FIGURE 2.7

A comparison of (a) photolithography, (b) electron-beam, (c) x-ray lithography, and (d) ion-beam. (Based on Brodie, I., and J.J. Muray. 1982. *The Physics of Microfabrication*. New York: Plenum Press. With permission.[13])

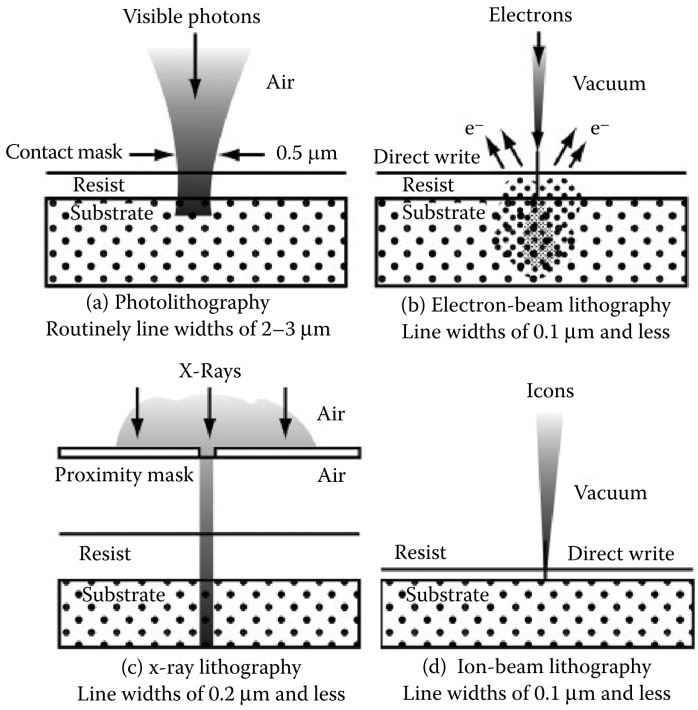

FIGURE 2.8

(a) Schematic of a synchrotron. (b) Grenoble synchrotron (http://www.esrf.eu).

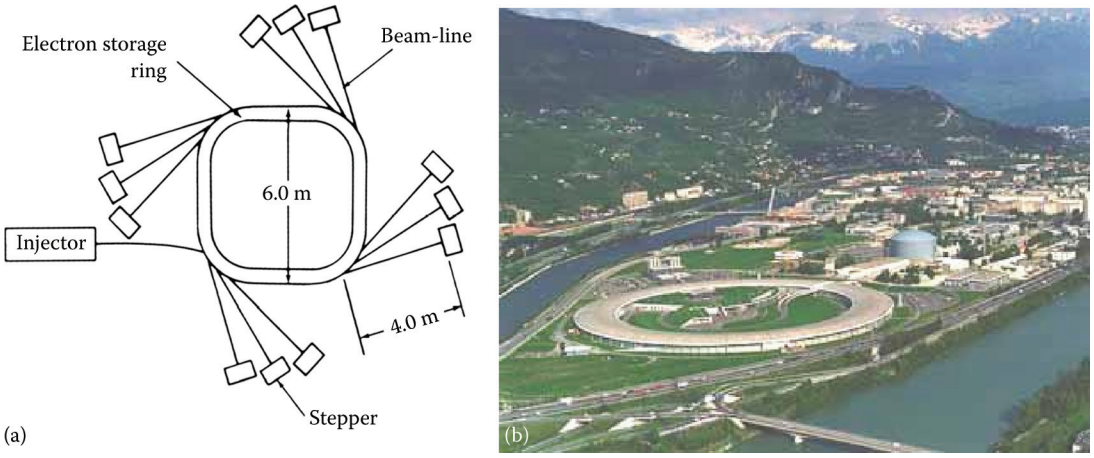

FIGURE 2.9

The LIGA process.

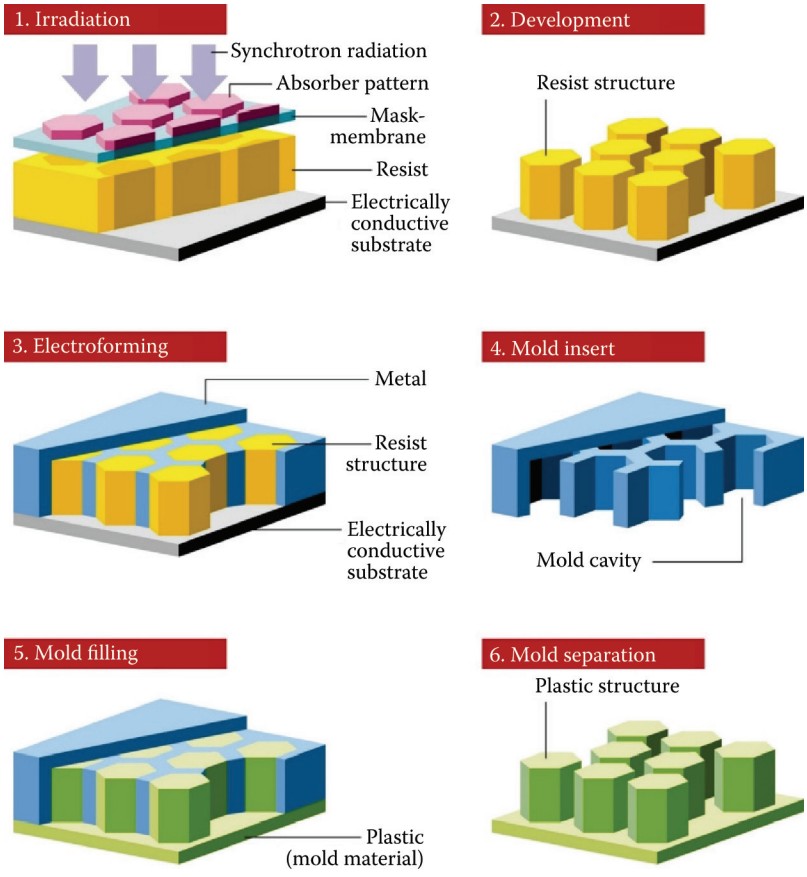

FIGURE 2.10

Ant with gear. (From Forschungszentrum Karlsruhe, Program Microsystem Technologies. With permission.)

FIGURE 2.11

LIGA structures obtained at IMM using an x-ray scanner enabling continuous tilt angles of the mask/substrate assembly. (Ehrfeld, W., and A. Schmidt. 1998. Recent developments in deep x-ray lithography. *J Vac Sci Technol* B16:3526–34.[19]) (Courtesy IMM.)

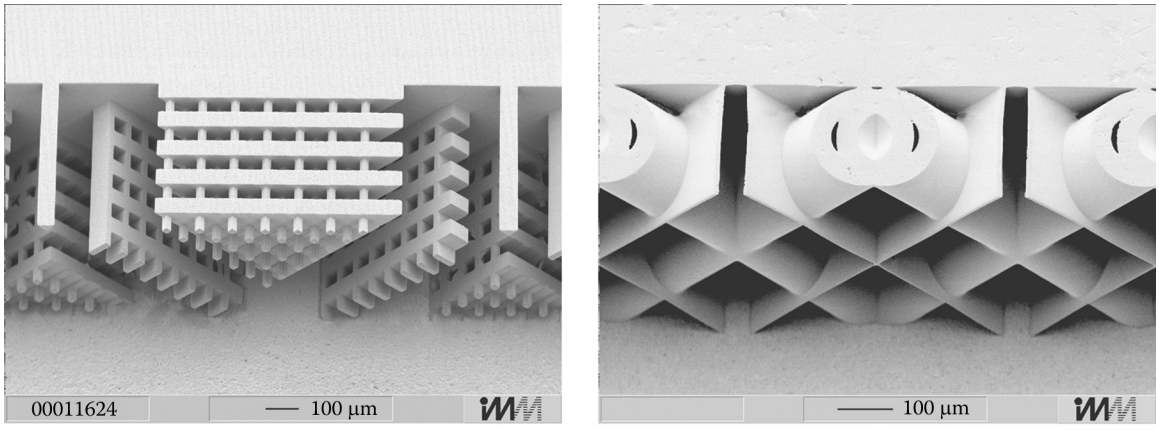

FIGURE 2.12

X-ray mask structure: Ta patterns on SiC or SiN membrane. The absorber Ta is 300 nm thick (stress ~ 0 MPa). Membrane SiC or SiN is 2 m thick (stress = 100 MPa ~ 200 MPa), 20 ~ 30 mm square. The minimum pattern width is 50 nm. Pattern position accuracy: $3\sigma < 30$ nm (http://www.ntt-at.com/products_e/x-ray_masks/index.html).

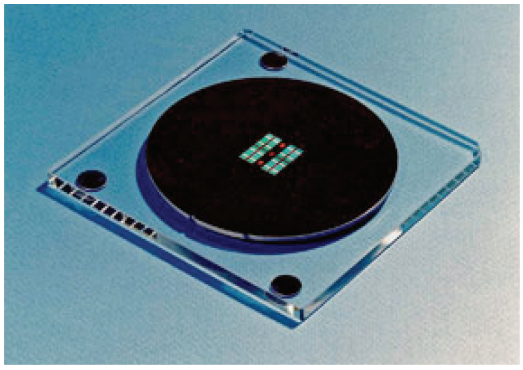

FIGURE 2.13

Fabrication of a silicon membrane-based x-ray mask with a gold absorber pattern. For use in high-aspect-ratio micromachining, the gold absorber layer must be between 5 and 15 μm. (Based on Brodie, I., and J.J. Muray. 1982. *The physics of microfabrication*. New York: Plenum Press. With permission.[13])

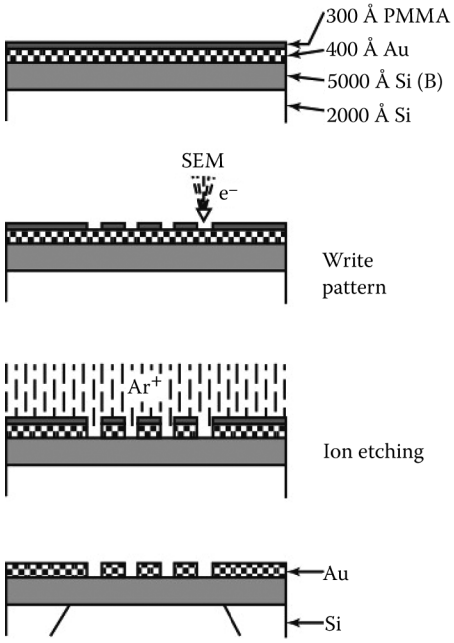

FIGURE 2.14

X-ray lithography with an electron-beam x-ray source. Inset, extent of penumbral effect calculated from geometric considerations. (Based on Brodie, I., and J.J. Muray. 1982. *The physics of microfabrication.* New York: Plenum Press. With permission.[13])

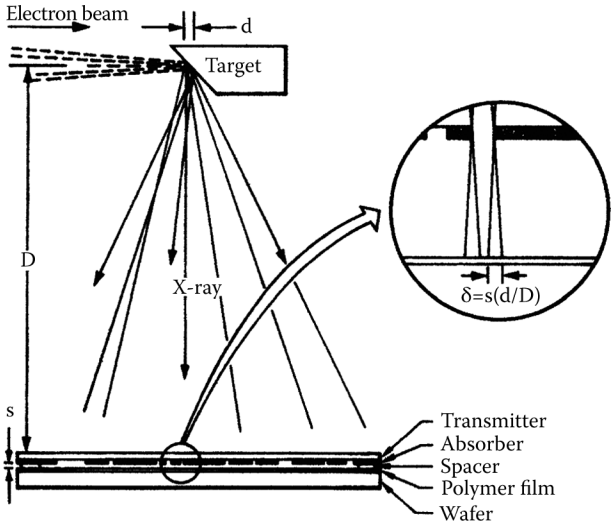

FIGURE 2.15

Scattering of the e-beam inside the resist and substrate and backscattering from the substrate exposing the resist over a greater area than the beam spot size.

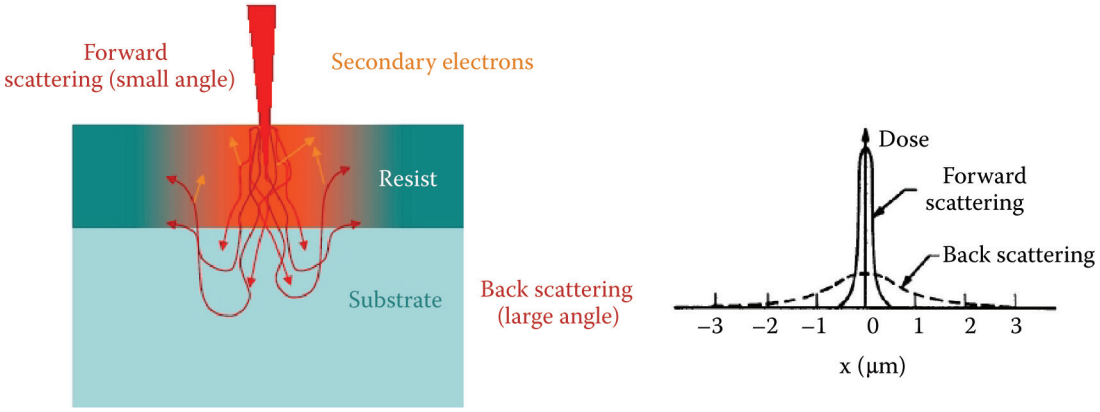

FIGURE 2.16

Proximity effect in direct write e-beam lithography.

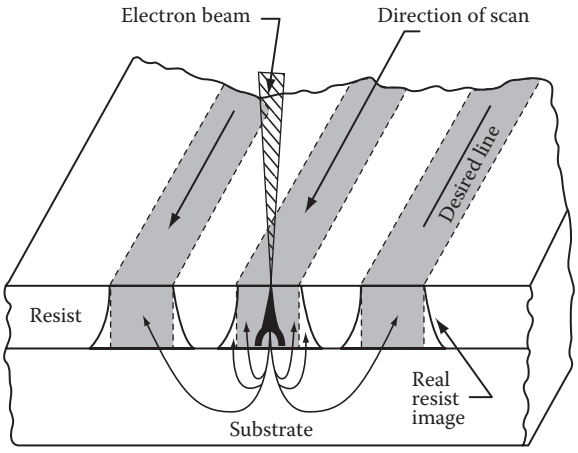

FIGURE 2.17

Photoemission, thermionic emission, and field emission.

Electron emission in a water bucket

THE THREE MECHANISMS used by field emission sources all basically involve emitting electrons and ions from a metal surface under the influence of a strong electric field.

Understanding these mechanisms is where the water bucket comes in.

In this analogy, the water level in a bucket represents the Fermi level—the highest occupied energy level in a cathode material. The work function is the energy required to get the water droplets (electrons) from the top of the liquid out of the bucket. This is the distance equivalent to the potential energy barrier.

In photoemission, photon energy excites electrons at the Fermi level of the cathode material and can impart enough kinetic energy to allow the electrons to escape from the bucket.

In thermionic emission, heat thermally excites the electrons, providing enough energy to boil the electrons off and out of the bucket.

In field emission a high electric field can thin the side of the bucket enough so that the electrons can tunnel through it.

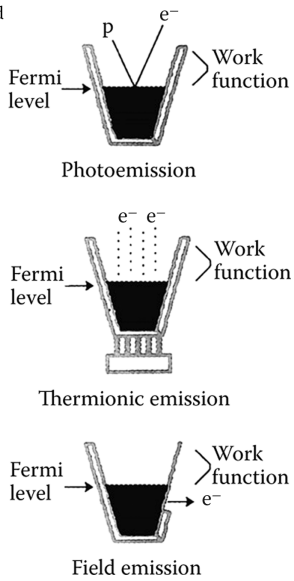

FIGURE 2.18

SE and CFE energy distributions.

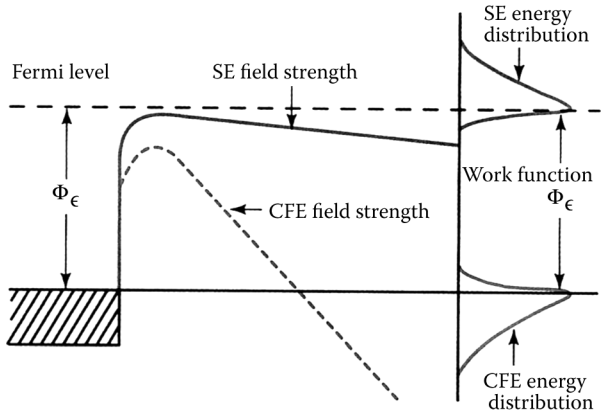

FIGURE 2.19

Scattering with angular limitation projection lithography or SCALPEL, a projection electron beam technique.

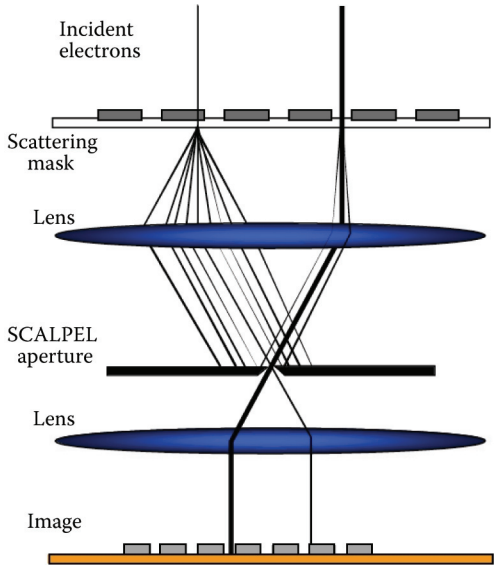

FIGURE 2.20

SCALPEL mask.

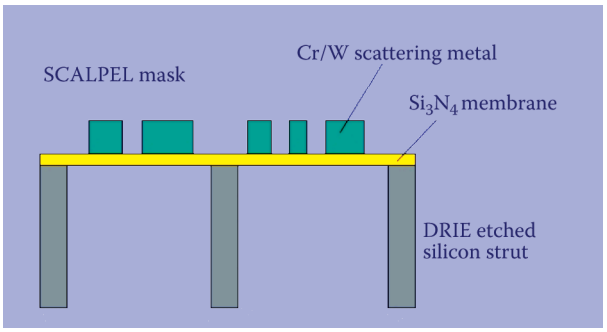

FIGURE 2.21

SCALPEL writing strategy involves step-and-scan writing.

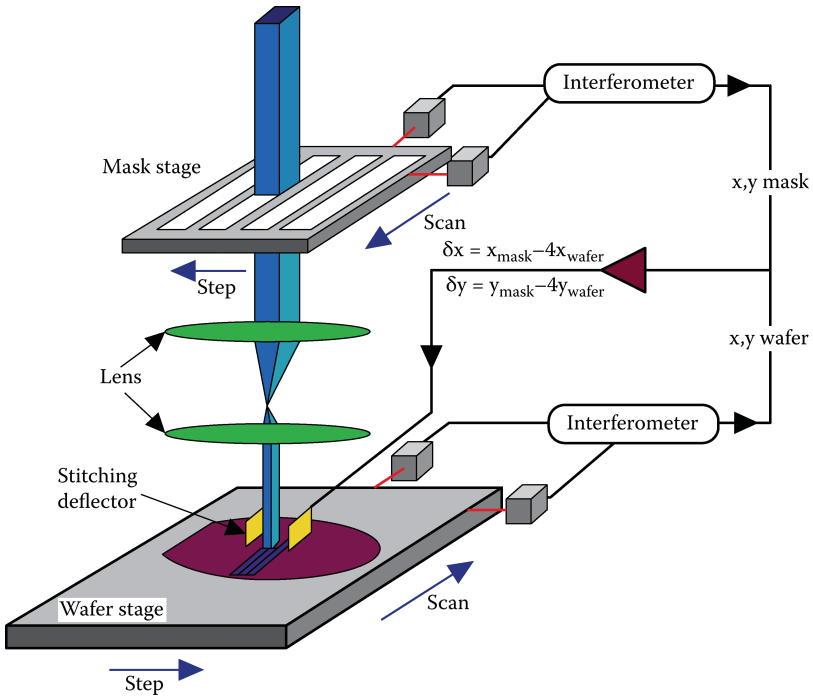

FIGURE 2.22

Array of focused electron writing beams operating at 300 eV or less. Setup (a) and detail of the lens system (b). (Redrawn from Zlatkin, A., and N. Garcia. 1999. Functional scanning electron microscope of low beam energy with integrated electron optical system for nanolithography. *Microelectron Eng* 46:213–17.[36])

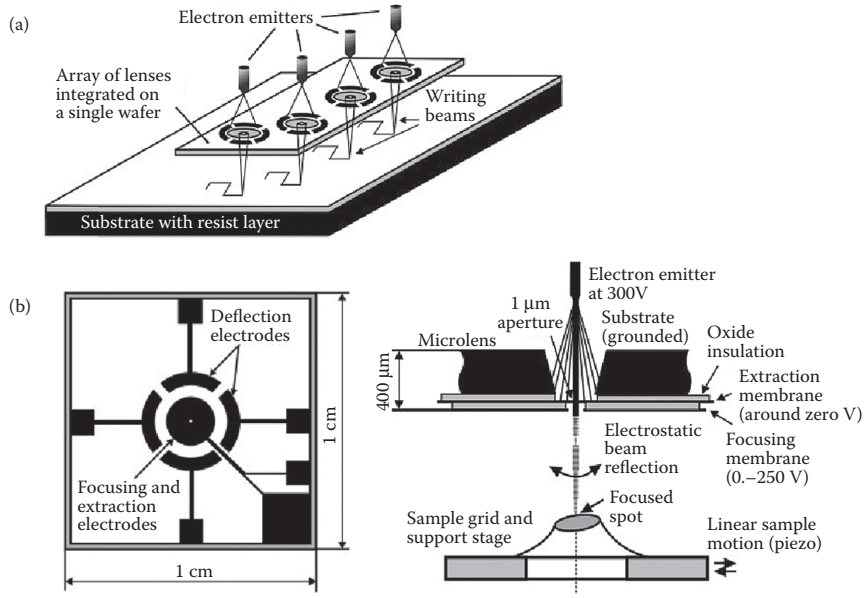

FIGURE 2.23

A microcolumn based on STM aligned field emission (SAFE) and arrayed microcolumn lithography. (From Editorial. 1993. Novel electron-beam lithography system being explored at Cornell's NNF. *Solid State Technol* 36:25–26. With permission.[37]) Acronyms are explained in the text.

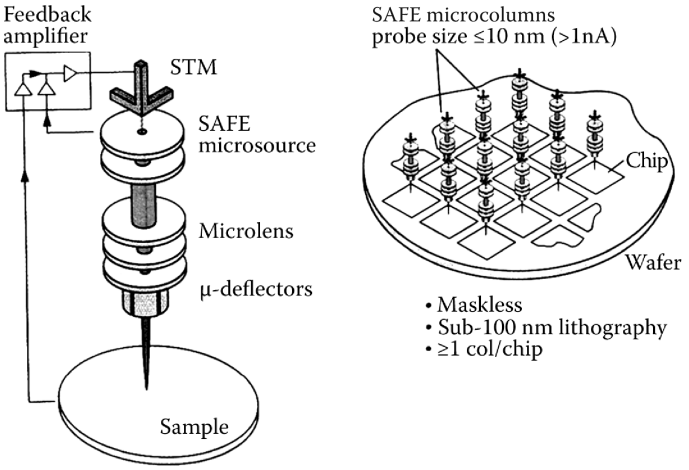

FIGURE 2.24

FIB deposition can produce features 200 nm or less in thickness. FIB milling can produce even finer results. Approximately 30 minutes of FIB time was required to produce this structure (http://fibics.com/Micromachining.html).

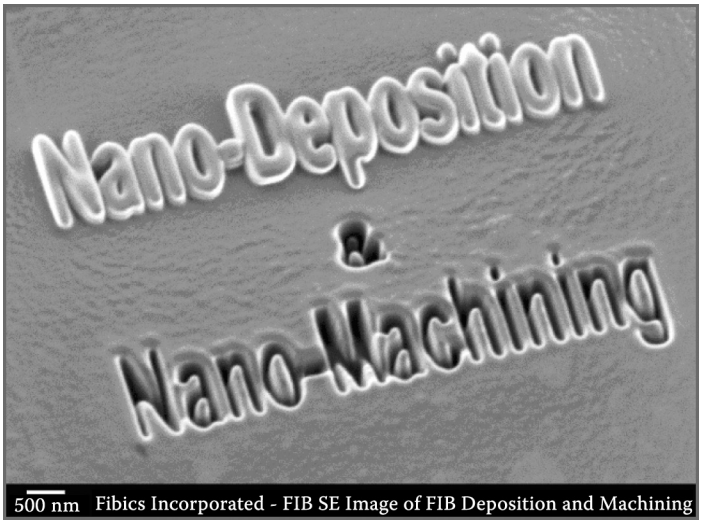

FIGURE 2.25

Ion projection lithography (IPL).

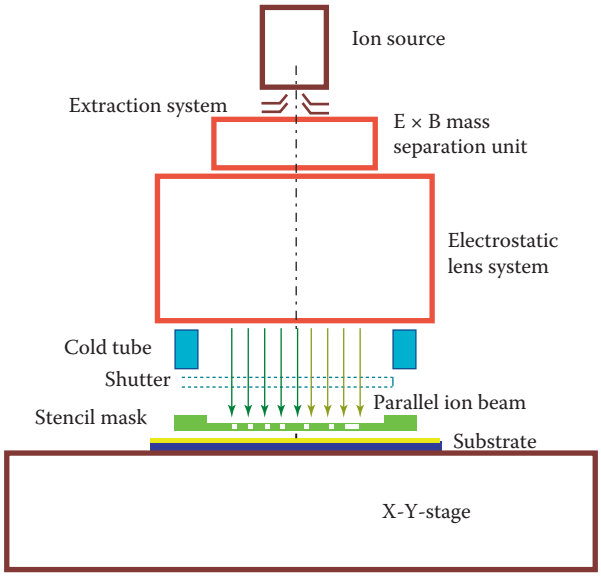

FIGURE 2.26

IPL mask 80-nm feature sizes etched into a Si membrane mask. The patterns were defined using a Leica VB6 EBL. (From http://www.cnf.cornell.edu/image.)

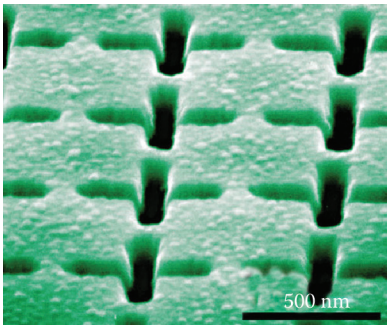

FIGURE 2.27

Schematic illustration of the nano imprint lithography (NIL). The technique is used here to pattern a metal film via liftoff.

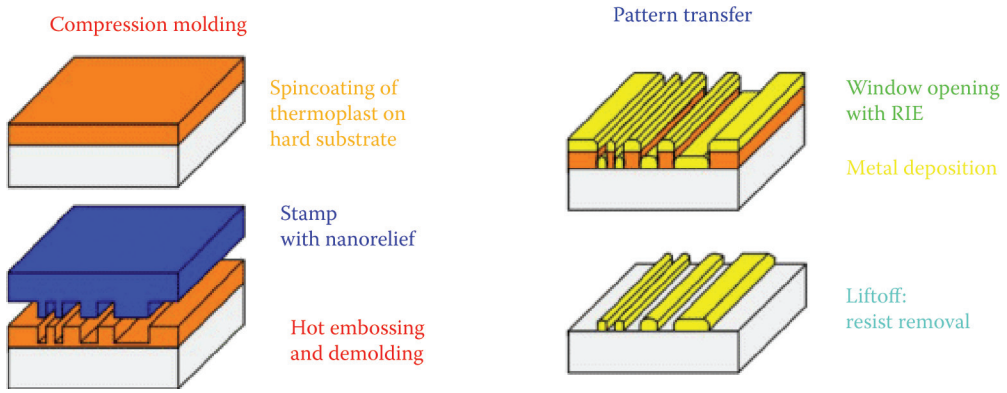

FIGURE 2.28

Schematic of step-and-flash imprint lithography (SFIL). (Colburn, M., S. Johnson, M. Stewart, S. Damie, T.C. Bailey, B. Choi, M. Wedlake, T. Michaelson, S.V. Sreenivasan, J. Ekerdt, and C.G. Wilson. 1999. Step and flash imprint lithography: a new approach to high-resolution patterning. *Proc SPIE* 3676:379–89.[47])

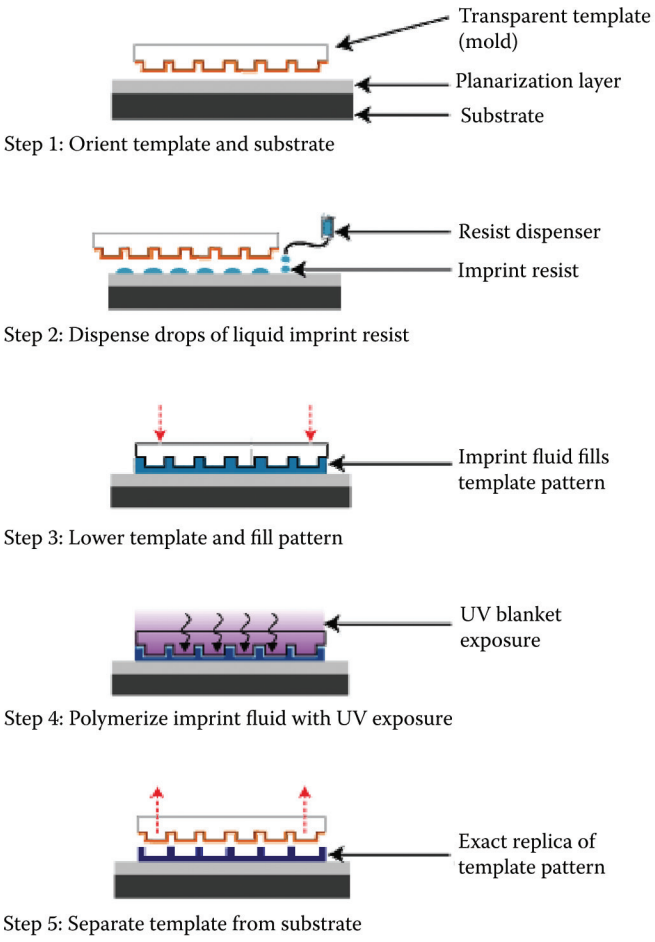

FIGURE 2.29

Usage domains of photocure (SFIL) and thermal nanoimprinting (NIL). (Based on a figure by Hitachi.)

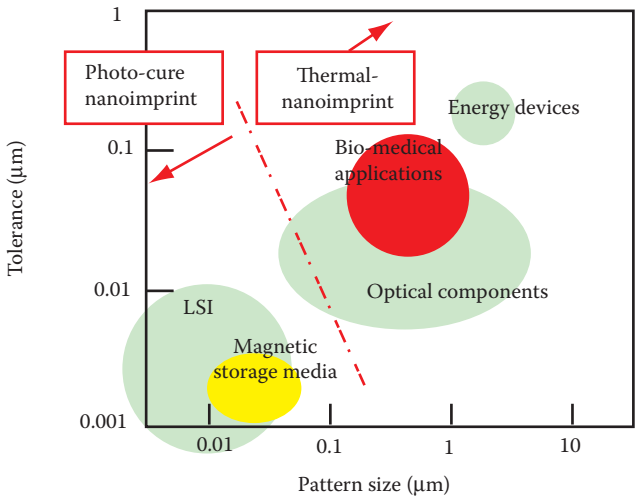

FIGURE 2.30

Schematic diblock copolymer phase diagram: f = volume fraction of *A* in *B*, χ = Flory-Huggins interaction parameter, N = diblock degree of polymerization. Known equilibrium mesophases are spheres, cylinders, gyroid, and lamellae, as well as the disordered (homogeneous) state at small interblock segregation strength (χN). (Diagram adapted from Matsen, M.W., and F.S. Bates. 1996. Unifying weak- and strong-segregation block copolymer theories. *Macromolecules* 29:1091–98.[62])

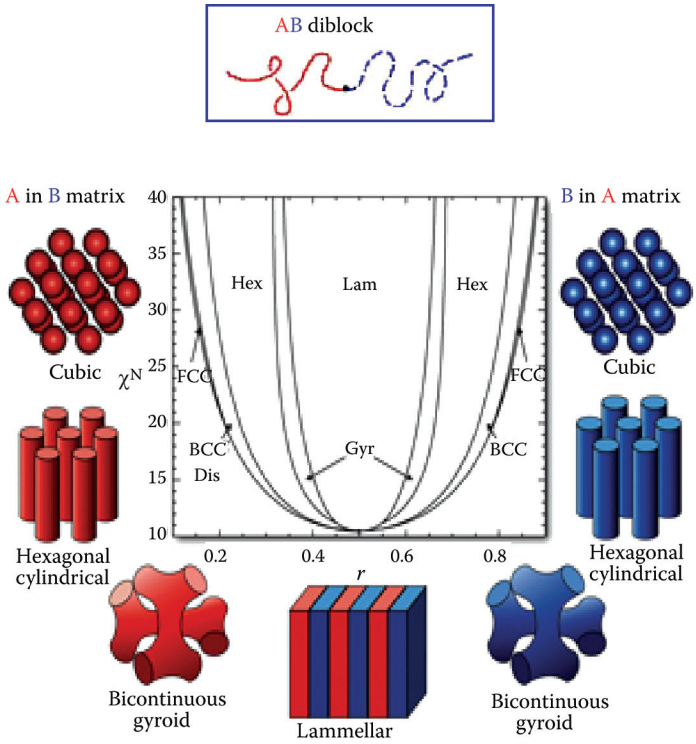

FIGURE 2.31

Traditional lithography compared with block copolymer lithography. Conventional lithography exposes a photoresist to ultraviolet light. A solvent etchant then removes the exposed part of the photoresist (for a positive type photoresist). Self-assembly patterning occurs when a diblock copolymer is heated, thereby separating the two polymers in the material into PMMA and polystyrene domains. The PMMA can then be selectively etched away, and the template of cylindrical holes can be transferred into the silicon dioxide. (Adapted from Stix, G. 2004. *Nano patterning: IBM brings closer to reality chips that put themselves together.* http://www.fractal.org/Fractal-Research-and-Products/Nano-patterning.htm.[65])

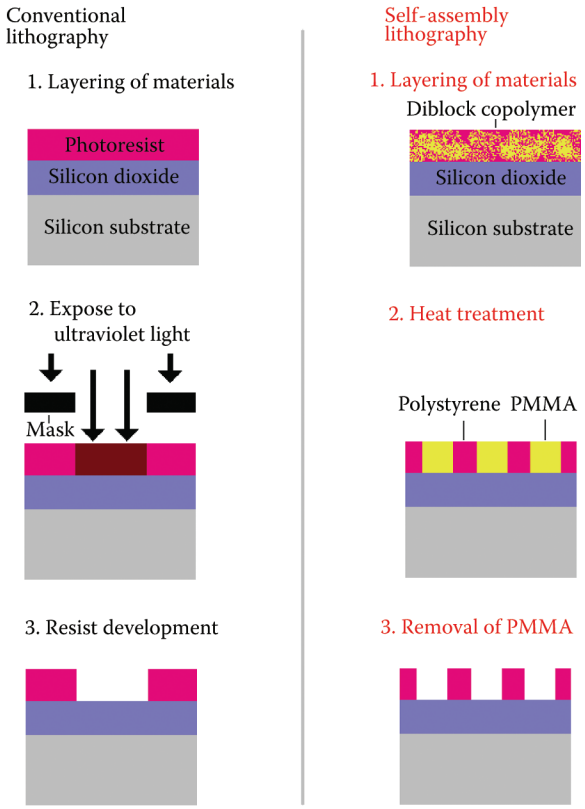

FIGURE 2.32

Flash memory: a layer of self-assembled silicon nanocrystals is inserted into an otherwise standard device as part of a novel IBM manufacturing process. (Based on Stix, G. 2004. *Nano patterning: IBM brings closer to reality chips that put themselves together.* http://www.fractal.org/Fractal-Research-and-Products/Nano-patterning.htm; and Black, C.T., R. Ruiz, G. Breyta, J.Y. Cheng, M.E. Colburn, K.W. Guarini, H.-C. Kim, and Y. Zhang. 2007. Polymer self assembly in semiconductor microelectronics. *IBM J Res Dev* 51: 605–33.[65,64])

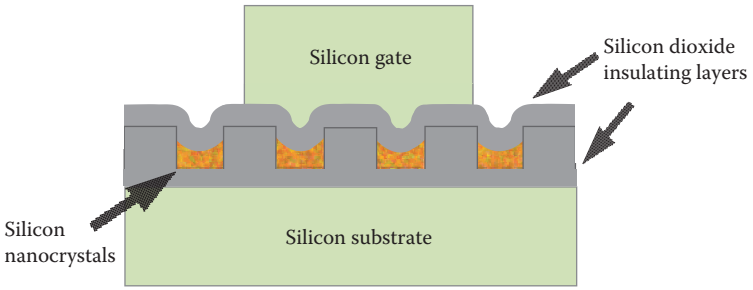

FIGURE 2.33

Patterned wettability of the surface causes the alignment of the nanodomains of a block copolymer. PMMA, polymethylmetacrylate; PS, polystyrene.

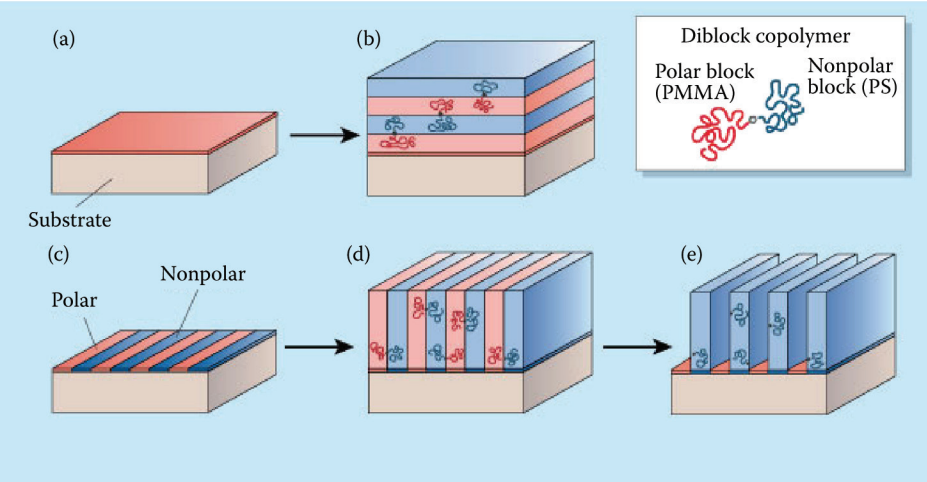

FIGURE 2.34

A Fresnel lens. (From http://xradia.com.)

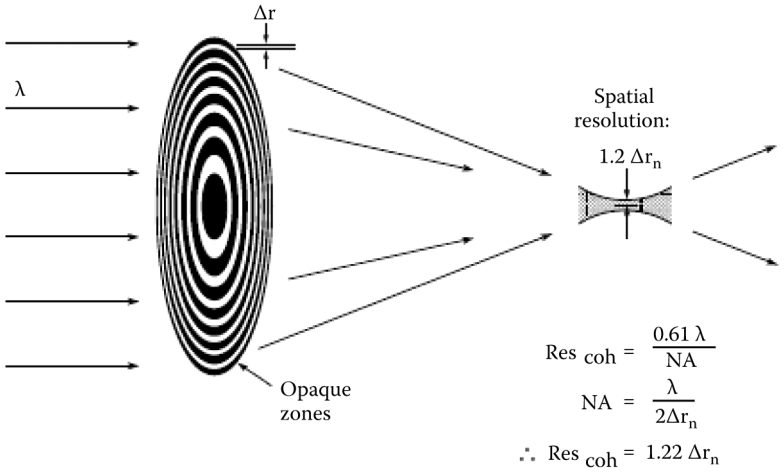

FIGURE 2.35

(a) Lumarray (http://www.lumarray.com) has demonstrated fully multiplexed ZPAL writing. (b) A laser beam is passed through a spatial filter and a collimating lens onto a digitally controlled programmable spatial light modulator (SLM), which replaces the photomask.[70,71]

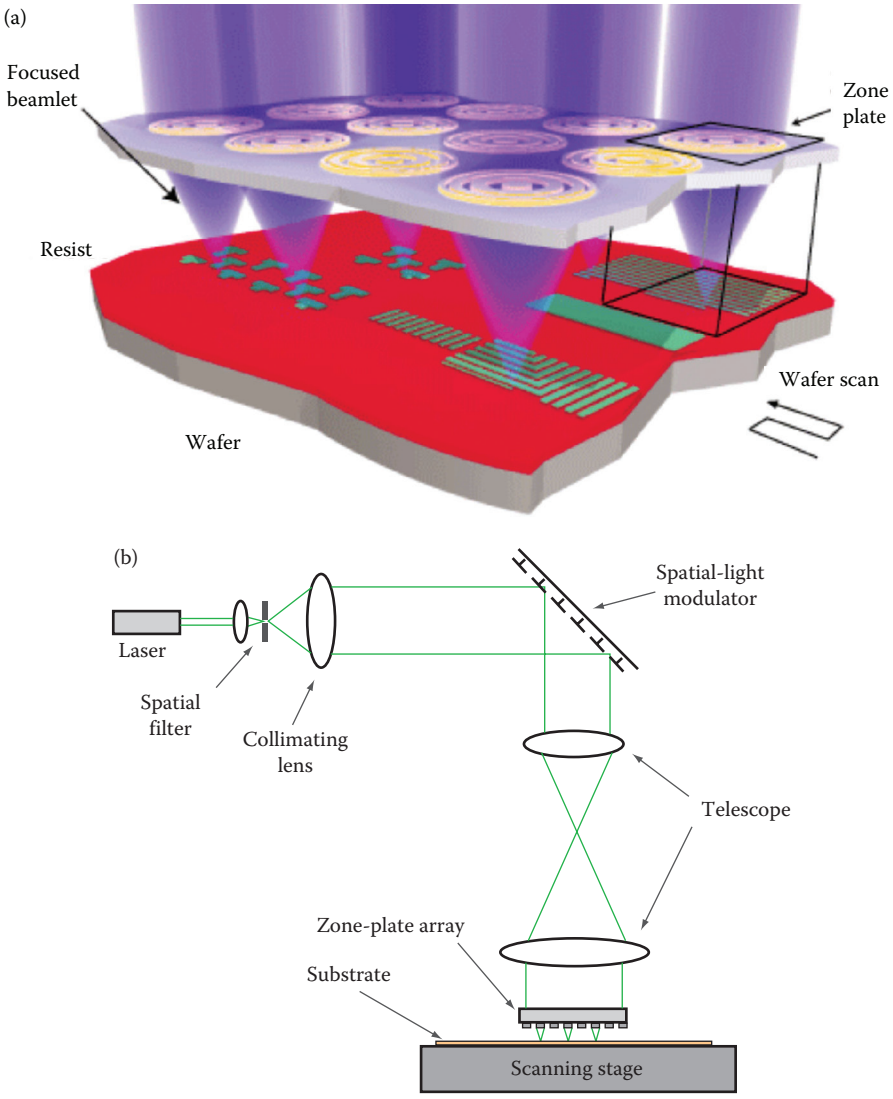

FIGURE 2.36

The entangled photon pair comes out from a point of the object plane, undergoes two-photon diffraction, and results in twice narrower point spread function on the image plane.

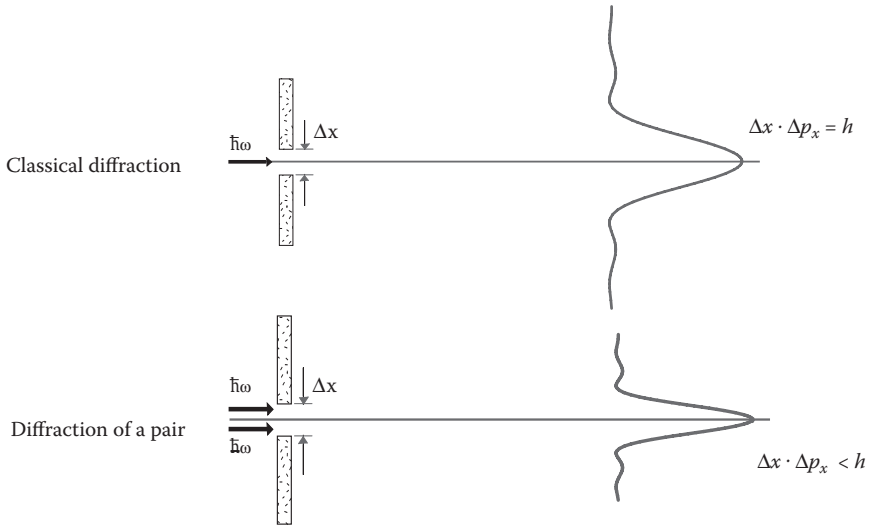

FIGURE 2.37

Two-photon 3D lithography. (a) Microspider array, the body of the spider is above the substrate; it is supported by eight 1-μm thick legs (http://www.laser-zentrum-hannover.de). (b) Venus micromodels on a human hair (http://www.laser-zentrum-hannover.de).

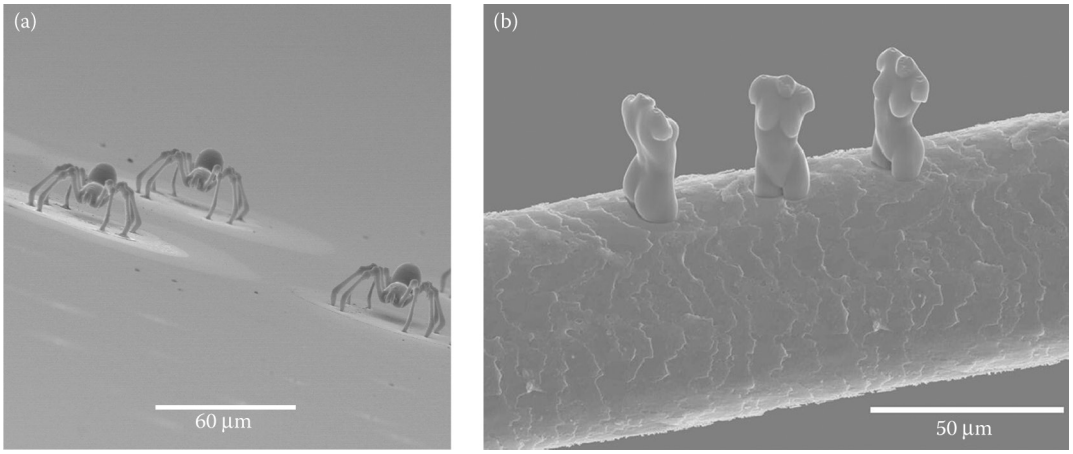

FIGURE 2.38

Schematic representation of plasmon printing showing glancing angle illumination using polarized visible light, producing enhanced resist exposure directly below the metal nanostructures in the mask layer (a), and the resulting pattern in the resist layer after development (b).

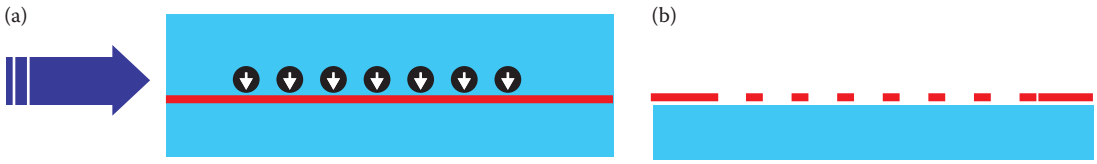

FIGURE 2.39

Nanotube mounted on the micromachined tip of a Si cantilever is used as a nanopencil for lithography of 20–10-nm lines (courtesy of Dr. M. Meyyappan, NASA Ames). SEM picture of nanotube mounted on tip of Si cantilever (http://cnst.rice.edu/pics.html).

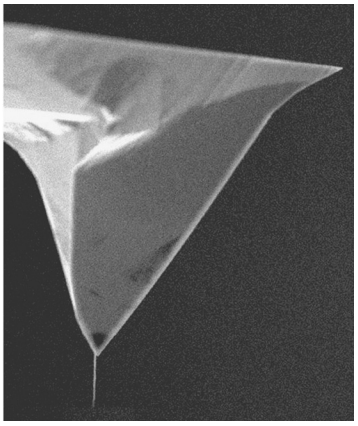

FIGURE 2.40

Schematic of AFM lithography on SiO_2 using a multilayered resist system. (a) Cross-section. (b) Exposure by drawing patterns into the ODS-SAM layer by current injection from an AFM probe. (c) First development step by HF etching to remove the SiO_2 just formed. (d) Second development step by TMAH etching to remove the a-Si in the exposed area. (e) Pattern transfer with HF to remove the thermal oxide in the exposed area. (f) Resist removal, i.e., removal of all the remaining a-Si in TMAH etch. (Based on Sugimura, H., O. Takai, and N. Nakagiri. 1999. Multilayer resist films applicable to nanopatterning of insulating substrates based on current-injecting scanning probe lithography. *J Vac Sci Technol* B17:1605–08.[87])

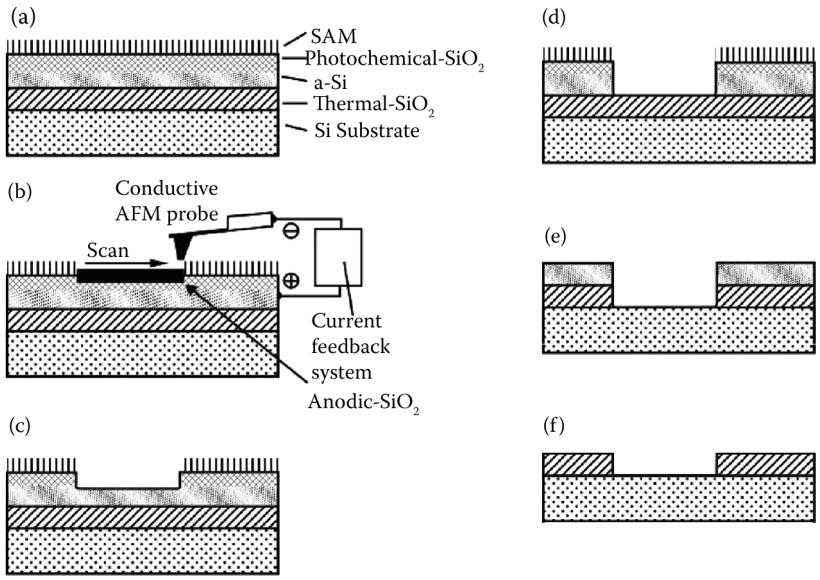

FIGURE 2.41

Line width versus dose for SAL601 resist using both EBL and SPL lithography systems. (Wilder, K., C.F. Quate, B. Singh, and D.F. Kyser. 1998. Electron beam and scanning probe lithography: a comparison. *J Vac Sci Technol* B16:3864–73.[89])

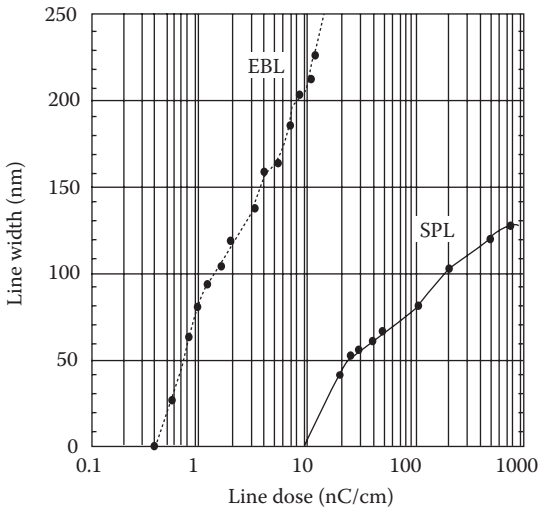

FIGURE 2.42

Spindt field emitter array. For its fabrication see Chapter 7, and for its application in a field emission display see Volume III, Chapter 10.

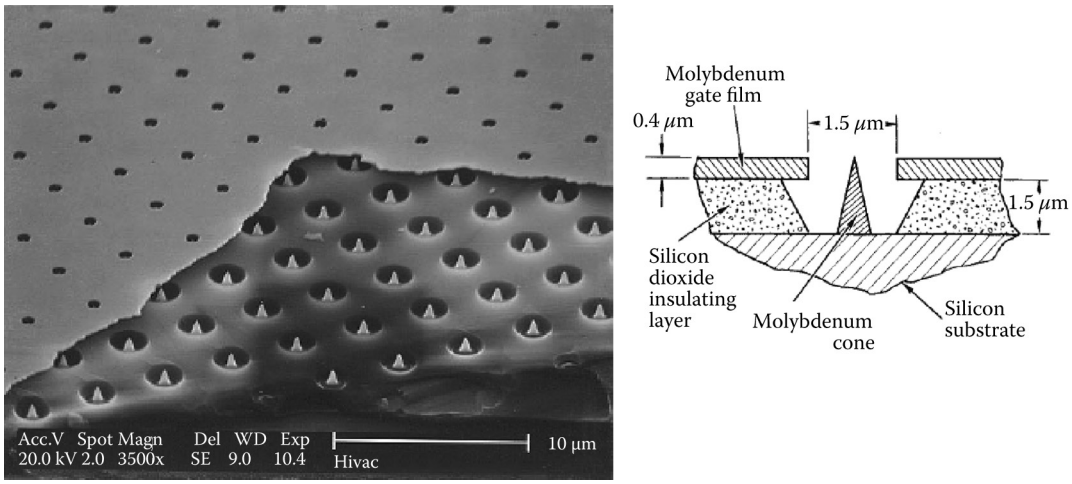

FIGURE 2.43

Atom manipulation for nanomatching. (a) A 60 × 48 Å STM image of four Pt adatoms assembled into a linear array on a Pt (111) surface. Pt atoms were herded four unit cells apart along a close-packed direction of the Pt (111) surface. (b) A 40 × 40 Å STM image of a compact array of seven Pt adatoms. (From Stroscio, J.A., and D.M. Eigler. 1991. Atomic and molecular manipulation with the scanning tunneling microscope. *Science* 254:1319–26. With permission.[95]) For more pictures of STM atom manipulation, visit http://www. almaden.ibm. com:80/vis/stm/gallery.html.

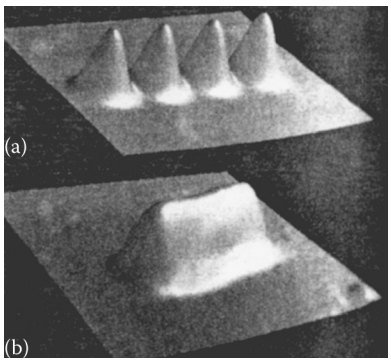

FIGURE 2.44

STM topographic images from a single Au atom to a linear chain of 20 atoms, arranged in single-atom increments from left to right. The images are cut from 20 separate scans, each taken with a sample bias voltage between 2.0 and 2.5 V and a tunneling current between 1.0 and 1.5 nA. Each chain has an apparent height between 2.4 and 2.7 Å. The chains between 12 and 20 atoms long were constructed and imaged with a tip different than the tip used to construct and image the other chains. (Wallis, T.M., N. Nilius, and W. Ho. Electronic density oscillations in gold atomic chains assembled atom by atom. *Phys Rev Lett* 89:236802-1–2-4.[97])

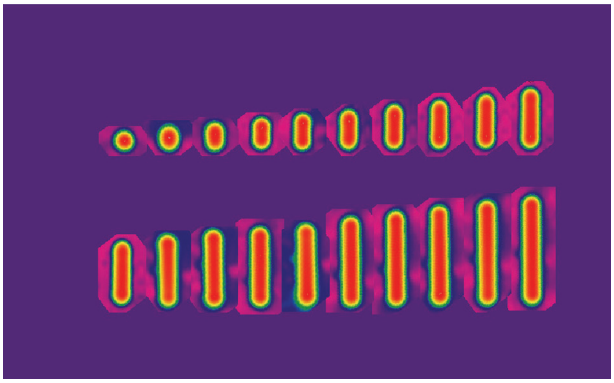

FIGURE 2.45

Assembly sequence and schematic for a structure consisting of a CuPc molecule and two Au_3 chains ($2Au_3$). All images were taken with V_{bias} = 1 V, I = 1 nA. (a) CuPc molecule (appears as a protruding four-lobe structure) on the NiAl surface together with seven Au atoms, which appear as round protrusions. Four of the atoms have been aligned along the same Ni trough. Image size is 74 Å by 74 Å. (b) One of the atoms has been manipulated along the Ni trough to create a Au_2 chain. (c) First Au_3 is created; another atom is positioned five Ni-Ni lattice sites (5 × 2.89 Å) away from Au_3, marking the starting position for another Au_3 chain. (d) A second Au_2 chain is created. (e) Assembly of the second Au_3 chain and the $2Au_3$ junction is completed. (f) Zoom-in image of the $2Au_3$ and CuPc molecule; the area of image is 47 Å × 47 Å. The image was taken with a tip modified by a CuPc molecule adsorbed on it. (g) The CuPc molecule has been moved into the junction between the two Au_3 chains. As is clear from the image, the molecule is adsorbed only on one of the chains. (h) The position of the molecule was adjusted by manipulating the leftmost lobe of the molecule in (g) toward the lower Au_3 chain. The molecule is adsorbed symmetrically between the two chains, forming CuPc@$2Au_3$. (The tip still has a CuPc molecule adsorbed on the apex.) (i) Image of same structure taken after removing the molecule adsorbed on the tip. The area corresponds to that of (e). (j) Schematic showing the relation between the internal molecular structure, adsorption geometry, and STM image. Black circles represent the Au atoms comprising the two Au_3 chains. (From Nazin, G.V., X.H. Qiu, and W. Ho. 2003. Visualization and spectroscopy of a metal-molecule-metal bridge. *Science* 302:77–81.[98])

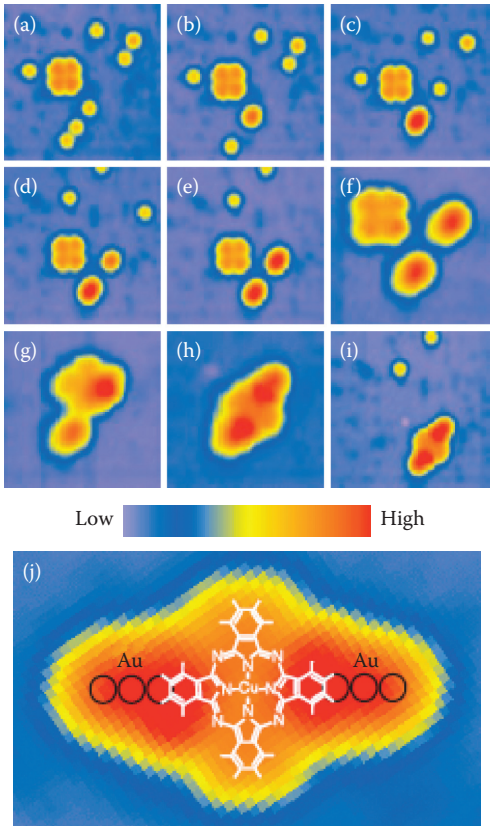

FIGURE 2.46

Dip pen nanolithography: transport of molecules to the surface via water meniscus (http://chemgroups.northwestern.edu/mirkingroup/dpn.htm).

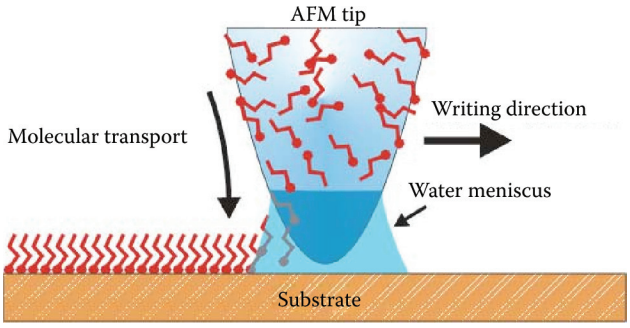

FIGURE 2.47

Diagram illustrating thermal dip pen nanolithography. When the cantilever is cold (a), no ink is deposited. When the cantilever is heated (b), the ink melts and is deposited onto the surface. (Image courtesy of Naval Research Laboratory, http://gtresearchnews.gatech.edu/newsrelease/tdpn.htm.)

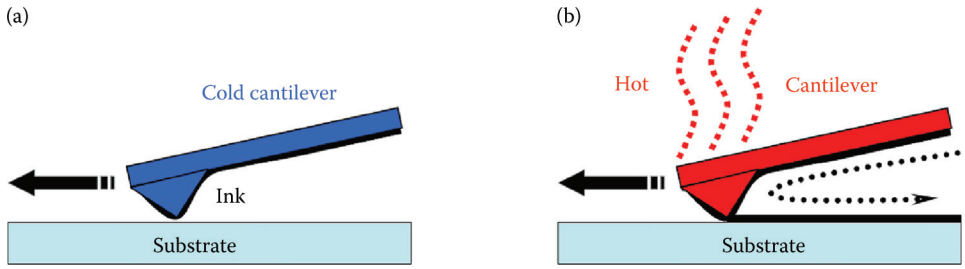

FIGURE 2.48

A topographic image of a surface scanned with a heated AFM cantilever tip for 256 s in each of four 500-nm squares. The cantilever temperature is shown for each of the four scans. No deposited material is observed from the two low-temperature scans. The scan at 98°C resulted in light deposition. Robust deposition occurred during the final scan when the cantilever temperature was 122°C. (Courtesy of Naval Research Laboratory.)

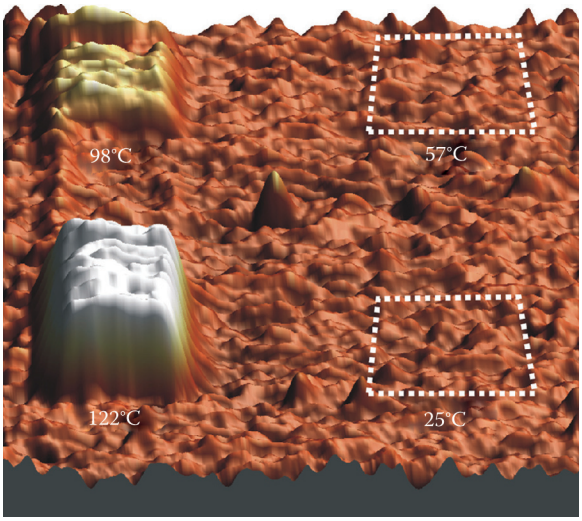

FIGURE 2.49

Recording a hologram. (From John G. Cramer.)

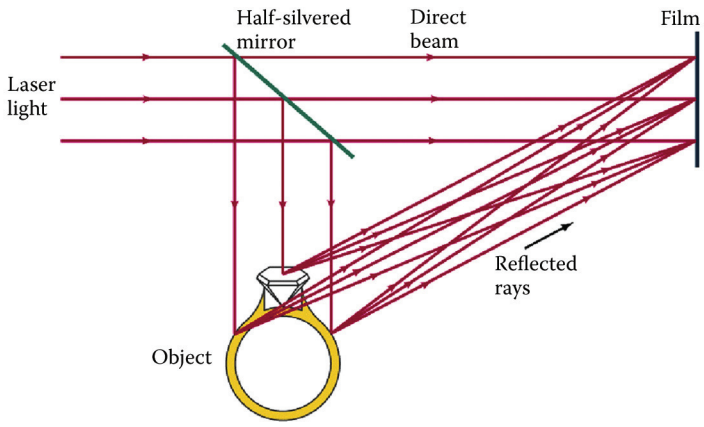

FIGURE 2.50

Basic arrangement for holographic lithography. (a) The photomask pattern forms a hologram in the polymer recording layer. (b) Using the illumination beam, the high-resolution holographic mask image is reconstructed into a printable masking layer in the resist-coated substrate. (From Brook, J., and R. Dandliker. 1989. Submicrometer holographic photolithography. *Solid State Technol* 32:91–94; and Omar, B., S. Clube, F. Hamidi, M.D. Struchen, and S. Gray. 1991. Advances in holographic lithography. *Solid State Technol* September:89–94.[108,109])

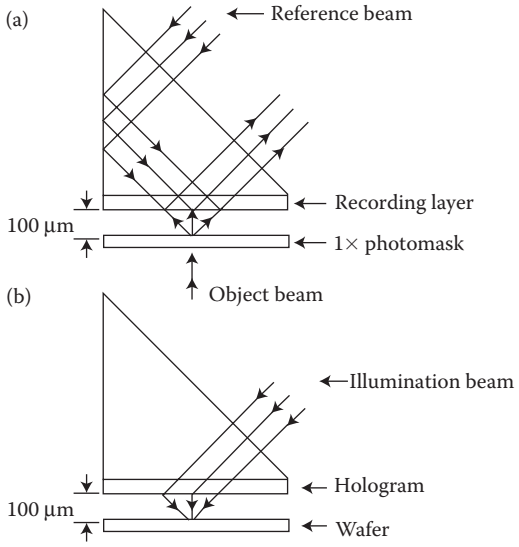

FIGURE 2.51

Polydimethylsiloxane (PDMS). (Sylgard 184, Dow Corning, http://www.dowcorning.com.)

- Low cost
- Easy fabrication
- Elastomeric/soft
- Moldable
- Surface chemistry
- Bonding
- Biocompatible

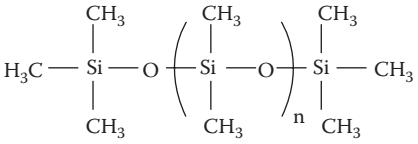

FIGURE 2.52

Making a PDMS mold. (Based on Xia, Y., and G.M. Whitesides. 1998. Soft lithography. *Angew Chem Int Ed* 37:550–75; and Xia, Y., and G.M. Whitesides. 1998. Soft lithography. *Ann Rev Mater Sci* 28:153–84.[113,114])

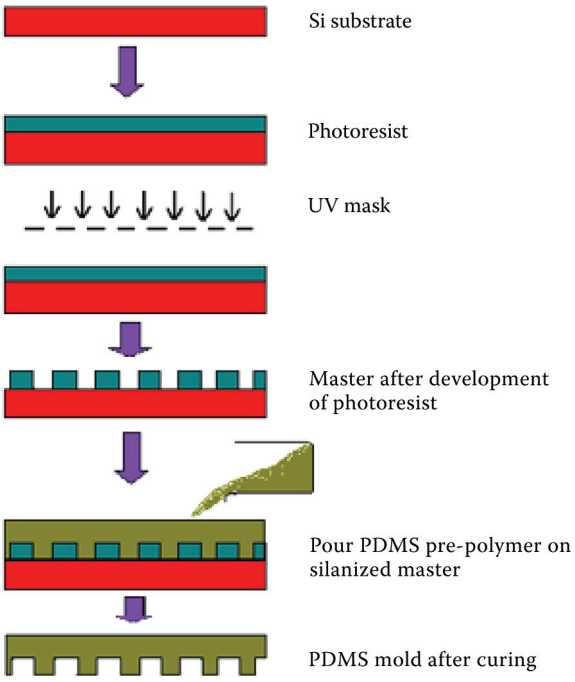

FIGURE 2.53

Microcontact printing of protein.

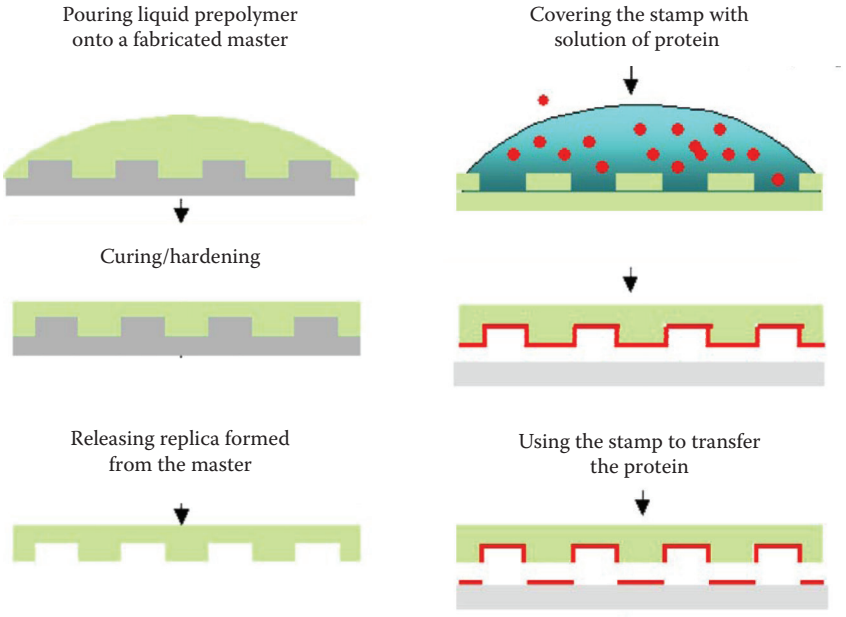

FIGURE 2.54

Schematic description of microtransfer molding (μ-TM). (Based on Xia, Y., and G.M. Whitesides. 1998. Soft lithography. *Angew Chem Int Ed* 37:550–75; and Xia, Y., and G.M. Whitesides. 1998. Soft lithography. *Ann Rev Mater Sci* 28:153–84.[113,114]) PU is prepolymer (polyurethane).

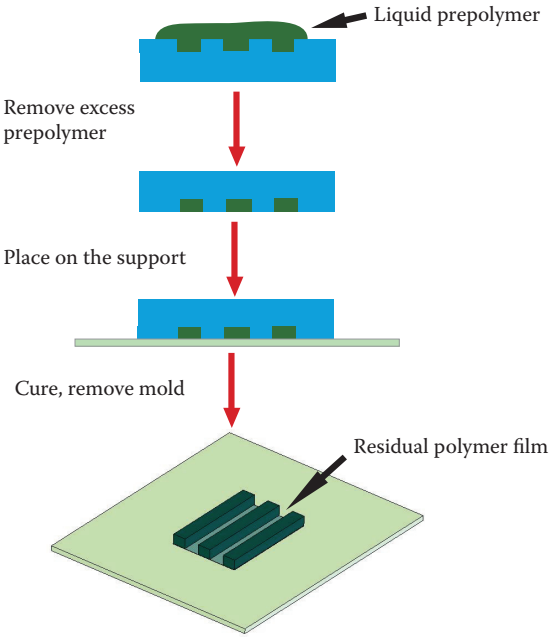

FIGURE 2.55

Curved glassy carbon structure. (Schueller, O.J.A., S.T. Brittain, and G.M. Whitesides. 1999. Fabrication of glassy carbon microstructures by soft lithography. *Sensors Actuators A* A72:125–39.[111] Courtesy of Dr. G.M. Whitesides, Harvard University.)

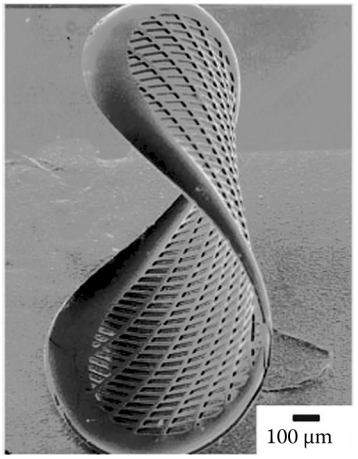

FIGURE 2.56

Schematic description of micromolding in capillaries (MIMIC). (Based on Xia, Y., and G.M. Whitesides. 1998. Soft lithography. *Angew Chem Int Ed* 37:550–75; and Xia, Y., and G.M. Whitesides. 1998. Soft lithography. *Ann Rev Mater Sci* 28:153–84.[113,114])